

Dust-acoustic solitary waves and double layers in a magnetized dusty plasma with nonthermal ions and dust charge variation

W. F. El-Taibany^{a)} and R. Sabry

Department of Physics, Faculty of Science-Damietta, Mansoura University, Damietta El-Gedida,
P.O. 34517, Egypt

(Received 6 April 2005; accepted 6 June 2005; published online 21 July 2005)

The effect of nonthermal ions and variable dust charge on small-amplitude nonlinear dust-acoustic (DA) waves is investigated. It is found that both compressive and rarefactive solitons exist and depend on the nonthermal parameter a . Using a reductive perturbation theory, a Zakharov–Kuznetsov (ZK) equation is derived. At critical value of a , a_c , a modified ZK equation with third- and fourth-order nonlinearities, is obtained. Depending on a , the solution of the evolution equation reveals whether there is coexistence of both compressive and rarefactive solitary waves or double layers (DLs) with the possibility of their two kinds. In addition, for certain plasma parameters, the solitary wave disappears and a DL is expected. The variation of dust charge number, wave velocity, and soliton amplitude and its width against system parameters is investigated for the DA solitary waves. It is shown that the incorporation of both the adiabatic dust-charge variation and the nonthermal distributed ions modifies significantly the nature of DA solitary waves and DA DLs. The findings of this investigation may be useful in understanding the ion acceleration mechanisms close to the Moon and also enhances our knowledge on pickup ions around unmagnetized bodies, such as comets, Mars, and Venus. © 2005 American Institute of Physics. [DOI: 10.1063/1.1985987]

I. INTRODUCTION

There has been a rapidly growing interest in dusty plasma physics not only because of dust being an omnipresent ingredient of our universe, but also because of its vital role in understanding different collective processes (mode modification, new eigenmodes, coherent structures, etc.) in astrophysical and space environments as well as in laboratory plasmas.¹ The consideration of charged dust grains in plasma does not only modify the existing plasma-wave spectra, but also introduces a number of new novel eigenmodes. One of these new eigenmodes are the dust-acoustic (DA) waves.^{2,3}

Highly charged massive dust grains presented in plasma may exhibit charge fluctuations in response to certain types of oscillations incorporated to the plasma.⁴ It has been shown that the dust-charge variation affects the characteristic collective motion of the plasmas.⁵ Therefore, it is important to study the effect of dust-charge variation on the nature of DA solitary waves. The consequent modifications in the collective properties of dusty plasma in response to the variation of charge were studied for various plasma systems. For example, Xie *et al.*⁶ derived DA solitons with varying dust charges and showed that only the rarefactive solitary waves exist when the Mach number lies within an appropriate regime depending on the system parameters. Moreover, the DA solitary waves and double layers (DLs) in dusty plasma with variable dust charge and two-temperature ions were studied by Xie *et al.*⁷ They have shown that both compressive and rarefactive solitons as well as DLs exist. Also, the amplitudes of the DA solitary waves become smaller and the

regime of the Mach number is extended wider for the variable dust-charge situation compared to the constant dust-charge situation. Later, El-Labany and El-Taibany^{8,9} and El-Labany *et al.*¹⁰ studied the DA waves under the combined effects of arbitrary streaming-ion beam, trapped ion distribution, two-temperature ion, dust-charge fluctuation, and dust fluid temperature in unmagnetized dusty plasmas. It is found that owing to the departure from the Boltzmann ion distribution to the trapped ion distribution, the dynamics of DA waves is governed by a modified Korteweg–de Vries equation. This equation admits a stationary DA solitary wave solution, which has stronger nonlinearity, smaller amplitude, wider width, and higher propagation velocity than the case when the adiabatic ions are involved. The effect of two-temperature ion is found to provide the possibility for the coexistence of rarefactive and compressive DA solitary structure and DLs. Although the dust fluid temperature increases the soliton amplitude, the dust-charge fluctuation does the opposite effect.

However, observations of space plasmas indicate the presence of nonthermal ion populations. Nonthermal ions from the Earth's bow shock have been observed by the Vela satellite,¹¹ as well as in and around the Earth's foreshock.¹² The automatic space plasma experiment with a rotating analyzer (ASPERA) on the Phobos satellite has detected nonthermal ion fluxes from the upper ionosphere of Mars.¹³ Closer to the Earth, fast nonthermal ions have been recently observed by the Nozomi satellite in the vicinity of the Moon.¹⁴ It appeared from the observations that the nonthermal ions have a partial ring structure in the velocity phase space. The mechanism suggested for the formation of a partial ring structure for nonthermal ions is that some of the solar wind ions are deflected in the close vicinity of the

^{a)} Author to whom correspondence should be addressed. Electronic mail: eltaibany@hotmail.com or eltaibany@yahoo.co.uk

Moon. Such deflected ions have large velocities (the bulk velocity of the solar wind) and they move by the force of the electric field and gyrate about the magnetic lines.¹⁴ Cairns *et al.*¹⁵ have considered a plasma consisting of nonthermal electrons, with the excess of energetic particles and cold ions, and have shown that it is possible to obtain both positive (compressive) and negative (rarefactive) solitary waves. Later, Mamun¹⁶ studied the instability of obliquely propagating DA solitary waves in a magnetized nonthermal dusty plasma. He used the small- k perturbation expansion¹⁷ to study the instability through the Zakharov–Kuznetsov (ZK) equation describing the plasma system.

Zhang and Xue¹⁸ investigated the combined effects of the adiabatic dust-charge variation and nonthermal ions on DA solitary structures in magnetized dusty plasmas using ion-charging current similar to that corresponding to the Boltzmann-distributed ones, which are not appropriate to describe the dust charging process in the presence of nonthermal ion. Ghosh *et al.*¹⁹ studied the properties of one-dimensional nonlinear DA wave in magnetized dusty plasmas with variable charges, neglecting the nonthermal ions. Later, Ghosh *et al.*²⁰ presented, for the first time, the appropriate ion-charging current based on the orbit-motion-limited (OML) approach.^{1,4,21} Depending on the nonthermal parameter, they stated that there is a growth of the DA wave instead of the usual damping. Using the reductive perturbation method,²² Zhang and Xue²³ derived a Korteweg–de Vries–Burger equation governing the dust-acoustic shock wave. They studied numerically the effect of the external magnetized field, nonadiabatic dust-charge fluctuation, and nonthermally distributed ions on DA shock wave in dusty plasmas.

Most studies used charging currents independent of the magnetic field,^{23,24} assuming that the dust grain radius is much smaller than the electron gyroradius. For a plasma laboratory that uses weak magnetic fields, this condition may be appropriate. However, the charging of dust grains in a magnetic field has been investigated in connection with the charging of satellites and rockets in Earth's ionosphere and magnetosphere.^{4,25} The presence of an external magnetic field makes a dusty plasma anisotropic, i.e., charging currents to a spherical dust grain is different in different directions. However, in the presence of a very strong magnetic field, the orbits of the magnetized plasma particles are confined to one dimension along the field lines, as if they are “glued” to the magnetic-field lines. Hence, the perturbed field does not come into play, and the problem of charging currents becomes independent of the magnetic field.²⁶ Tsyrovich *et al.*²⁷ cleared that when the magnetic field becomes larger than a critical value (about 4 kG), the electron gyroradius equal the electron collection radius on dust grains. Only fast-magnetized electrons would be involved in the charging process, while a fraction of low-energy electrons would be reflected backwards along the magnetic-field direction. Hence, the cross section for magnetized electrons is changed, resulting in the lowering of the electron current by a factor of 4 compared to that in the absence of a magnetic field. In addition, at this value of the magnetic-field strength, the ion gyroradius is still much larger than the ion dust at-

traction size, the ions will be attracted to the dust grain with approximately the same rate, and the ion current on the grain will then remain the same as in an unmagnetized plasma. For a much stronger magnetic field in the plasma, the ion gyroradius becomes smaller than the dust size. Here, both the electron and ion currents are modified due to the strong magnetization of the plasma particles. Tsyrovich *et al.*²⁷ treated numerically the problem of much stronger magnetic field with variational charged dusty plasma and reported the dependence of dust charge on the external magnetic-field strength as well as on the parameter $\bar{\mu} = \sqrt{\mu_i \beta}$, where $\beta = T_i/T_e$, $\mu_i = m_i/m_e$, and $m_i/m_e(T_i/T_e)$ is the ion-to-electron mass (temperature) ratio. They found that the dust charge in a strong magnetic field could be substantially larger (up to 12 times) than that in the absence of the magnetic field (or in a weak magnetic field). Later, Salimullah *et al.*²⁶ used the kinetic theory to examine the currents of electrons and ions to a spherical dust grain in a uniform strongly magnetized dusty plasma. They found that the external magnetic field reduces the charging current, thereby decreasing the dust-charge fluctuation damping of a low-frequency electrostatic wave in a dusty plasma.

On the other hand, Zakharov and Kuznetsov²⁸ made the first attempt to model a soliton in a magnetized three-dimensional system. They obtained a three-dimensional differential equation, which is known as the ZK equation. Mamun *et al.*²⁹ investigated the properties of the multidimensional electrostatic solitary waves in magnetized nonthermal dusty plasmas, but they did not consider the dust-charge variation. Recently, El-Labany *et al.*³⁰ studied the contribution of higher-order nonlinearity to nonlinear DA solitary waves in warm magnetized three-component dusty plasmas comprised of variational charged dust grains, isothermal ions, and electrons. Considering the response of the charging currents to the ambient magnetic field, they have reduced the basic set of fluid equations to the coupled-ZK- and ZK-type equations. Our objective in this paper is to study, qualitatively, the propagation characteristics of nonlinear DA waves in a collisionless, three-component magnetized dusty plasma consisting of warm variational charged dust grains, nonthermal ions, and isothermal electrons.

The paper is organized as follows. The basic equations describing the dusty plasma system under consideration, incorporating the contribution from the variable dust charge, are given in Sec. II. In Sec. III, the dependence of the dust charge on the plasma parameters, especially the relation of the dust-charge variation to the plasma potential, is obtained using the current balance condition. In Sec. IV, using a reductive perturbation technique,²² the DA solitary structures are studied with the inclusion of a number of important effects such as adiabatic variation of dust grain charges and nonthermal ions. In Sec. V critical cases for the system are discussed and a modified ZK equation with third-order fourth-order, and mixed nonlinearities is obtained. Their solutions are also discussed. Section VI is devoted to the conclusion.

II. BASIC EQUATIONS

The dusty plasma, we are studying, consists of three components: extremely massive-highly negatively charged dust grains, isothermal electrons, and nonthermal ions, in the presence of an external magnetic field $\mathbf{B} = B_0 \hat{x}$. Charge neutrality at equilibrium reads

$$n_{io} = n_{eo} + Z_{do} n_{do}, \quad (1)$$

where n_{io} , n_{eo} , and n_{do} are the unperturbed ion, electron and dust number densities, respectively, and Z_{do} is the unperturbed number of charges residing in the dust grain and measured in units of the electron charge.

For three-dimensional low-frequency DA motions, we have the following nondimensional equations:³⁰

$$\frac{\partial n_d}{\partial t} + \nabla \cdot (n_d \mathbf{u}_d) = 0, \quad (2)$$

$$\frac{\partial \mathbf{u}_d}{\partial t} + (\mathbf{u}_d \cdot \nabla) \mathbf{u}_d - Z_d \nabla \phi + Z_d (\mathbf{u}_d \times \Omega \hat{x}) + \frac{5}{3} \frac{\sigma}{n_d^{1/3}} \nabla n_d = 0, \quad (3)$$

$$\nabla^2 \phi = Z_d n_d + n_e - n_i, \quad (4)$$

where n_j and \mathbf{u}_d refer to the number density of the j th species ($j=e$ for electrons, i for ions, d for dust) and fluid velocity of the dust grain, respectively. The densities of electrons and ions are normalized by $Z_{do} n_o$, the dust grain density is normalized by n_o , and Z_d is normalized by Z_{do} . The space coordinates $[x, y, z]$, time t , dust-cyclotron frequency Ω , velocity \mathbf{u}_d , and electrostatic potential ϕ are normalized by the Debye length $\lambda_{Dd} = (T_{\text{eff}}/4\pi Z_{do} n_{do} e^2)^{1/2}$, the inverse dust plasma frequency $\omega_{pd}^{-1} = (m_d/4\pi Z_{do} n_{do} e^2)^{1/2}$, ω_{pd} , the DA speed $C_d = (Z_{do} T_{\text{eff}}/m_d)^{1/2}$, and T_{eff}/e , respectively, where $T_{\text{eff}} = [Z_{do} n_{do} T_i T_e / (n_{io} T_e + n_{eo} T_i)]$. Because of the negation of the electron inertia, the electron density is governed by the Boltzmann distribution as

$$n_e = \frac{n_{eo}}{Z_{do} n_{do}} \exp(\beta s \phi) = \nu \exp(\beta s \phi), \quad (5)$$

where $s^{-1} = T_i/T_{\text{eff}} = \nu\beta + \mu$, $\mu = n_{io}/Z_{do} n_{do}$, and $\nu = n_{eo}/Z_{do} n_{do}$. Also, we define $\sigma = T_d/Z_{do} T_{\text{eff}}$.

As the ions are assumed to be nonthermally distributed,¹⁵ a possible three-dimensional equilibrium-state ion velocity distribution function satisfying the collisionless Vlasov equation with a population of fast (energetic) particle is given by

$$F_i(v_i) = F_i(v_x, v_y, v_z) = \frac{n_{io}}{(1+3a)} \frac{1}{(2\pi V_{ii}^2)^{3/2}} \left[1 + 4a \left(\frac{v_x^2}{2V_{ii}^2} + s\phi \right)^2 \right] \times \exp \left[- \left(\frac{v_x^2 + v_y^2 + v_z^2}{2V_{ii}^2} + s\phi \right) \right], \quad (6)$$

where a is the ion nonthermal parameter which determines the number of fast (energetic) ions, v_x , v_y , and v_z are the x , y and z components of the ion velocity v_i , and $V_{ii}^2 = \sqrt{T_i/m_i}$ is the ion thermal velocity. The steady-state one-dimensional

ion velocity distribution with a population of fast ion (with $v_x = v_i$ and $\phi = 0$) can be obtained by the integration of the distribution function (6) over the velocities v_y and v_z .¹⁵ Furthermore, if one puts $a=0$, one can reach the steady-state Maxwellian ion distribution function. For a nonzero potential, the integration of the distribution function, (6), will give the following ion number density:¹⁵

$$n_i = \int F_i(v_i) d^3 v_i = \mu \left[1 + \frac{4as\phi(1+s\phi)}{1+3a} \right] \exp(-s\phi). \quad (7)$$

III. CHARGING OF DUST GRAINS

Dust particles are charged due to a variety of processes including the bombardment of the dust grain surface by background plasma electrons, ions and incident ion beams, photoelectron emission by UV radiation, ion sputtering, secondary-electron production, etc.¹ In low-temperature plasmas, dust particles are mainly negatively charged particles when any plasma electrons hitting the surface of the dust grains are attached to it and simply lost from the background plasma.¹ In this paper we use the orbital-motion-limited (OML) approach^{1,4,21} to describe the charging of the dust grains. The electron and ion currents to the dust grains are given by

$$I_j = q_j \int_{R_j} \sigma_{sj}(v_j, \phi_d) v_j F_j(v_j) d^3 v_j, \quad (8)$$

where R_j is the domain of integration in the j -species velocity space, $\sigma_{sj} = \pi r^2 (1 - 2q_j \phi_d / m_j v_j^2)$ is the effective dust grain collisional cross section, q_j is the electric charge of the j -species of the plasma particles, $\phi_d = q_d / \tilde{C}$ is the dust surface potential relative to the plasma potential ϕ , q_d is the dust charge, and \tilde{C} is the capacitance of the spherical dust grain of average radius r .¹

As it is assumed that the electrons are Maxwellian, substituting the Maxwellian velocity distribution of electrons in (8) and then integrating, for spherical dust grains with radius r , we get the following expression for electron current:^{1,6,8}

$$I_e = -e\pi r^2 (8T_e / \pi m_e)^{1/2} n_{eo} \exp[s\beta(\psi + \phi)]. \quad (9)$$

Similarly substituting (6) into (8) and then integrating, we get the following expression for ion current:²⁰

$$I_i = e\pi r^2 (8T_i / \pi m_i)^{1/2} \frac{n_{io}}{(1+3a)} \exp \left[- (s\phi) \left\{ \left(1 + \frac{24a}{5} \right) + \frac{4as\phi}{3} (4 + 3s\phi) - s\psi \left[\left(1 + \frac{8a}{5} \right) + \frac{4as\phi}{3} (2 + 3s\phi) \right] \right\} \right], \quad (10)$$

where $\psi = e\phi_d / T_{\text{eff}} = -Z_d e^2 / \tilde{C} T_{\text{eff}}$ (at equilibrium $Z_d = Z_{do}$ and $\psi_o = -Z_{do} e^2 / \tilde{C} T_{\text{eff}}$). In Eq. (10), the parameter a arises due to the effect of nonthermal ions (putting $a=0$, we get the usual expression of ion current^{1,6,8} for Maxwellian ions). Hence, it is clear that the nonthermal ions also modify the ion current.

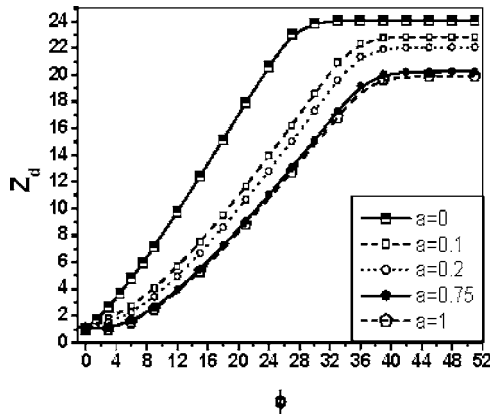


FIG. 1. Z_d is plotted against ϕ for different a values, where $\delta=10$ and $\beta=0.1$.

Here, we will focus on the case of adiabatic dust-charge variation in which $\omega_{pd} \ll \nu_{ch}$ (dust charging frequency); $\nu_{ch} = -[\partial(I_i + I_e)/\partial Q_d]/eZ_d$ at equilibrium, where Q_d is the dust-charge variable that can be determined through the charge-current balance equation^{1,4}

$$\frac{\partial Q_d}{\partial t} + (\mathbf{u}_d \cdot \nabla) Q_d = I_e + I_i. \tag{11}$$

Here, the magnetic field is strong enough; larger than the critical field at which the electron gyroradius equal the electron collection radius on dust grains [i.e., the electron current decreases by a factor 4 compared to that in the absence of a magnetic field], and the ion gyroradius is still much larger than the ion dust attraction size [i.e., the ion current on the grain will remain the same as in an unmagnetized plasma]. So, the reduction of the electron current means a decrease of the dust charge.^{26,27,30}

It is noticed also that the characteristic time for dust motion is of the order of tens of milliseconds for micrometer-sized grains,³ while the dust charging time is typically of the order of 10^{-8} s. Therefore, on the hydrodynamic time scale, the dust charge can quickly reach local equilibrium, at which the currents from the electrons and ions to the dust are balanced. The current balance equation reads^{1,30}

$$\frac{I_{eo}}{4} + I_{io} \approx 0.$$

Using Eqs. (9) and (10), the last equation becomes

$$\exp s\beta(\phi + \psi) = \frac{\alpha\delta \exp - (s\phi)}{1 + 3a} \left\{ \left(1 + \frac{24a}{5} \right) + \frac{4as\phi}{3}(4 + 3s\phi) - s\psi \left[\left(1 + \frac{8a}{5} \right) + \frac{4as\phi}{3}(2 + 3s\phi) \right] \right\}, \tag{12}$$

with $\psi_o = \psi(\phi=0)$ given as

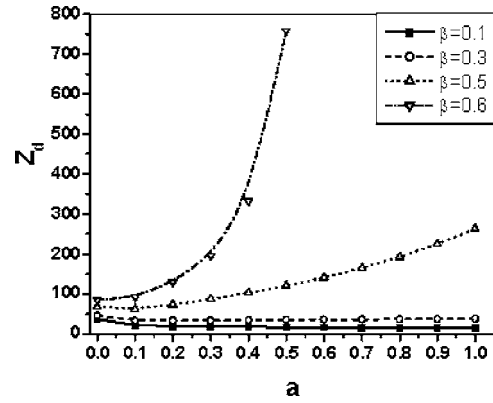


FIG. 2. Z_d is plotted against a for different β values, where $\delta=40$ and $\phi=10$.

$$\psi_o = \frac{1}{s\beta} \ln \left(\frac{\alpha\delta}{1 + 3a} \left\{ \left(1 + \frac{24a}{5} \right) - s\psi_o \left[\left(1 + \frac{8a}{5} \right) \right] \right\} \right), \tag{13}$$

where $\alpha = (\beta/\mu_i)^{1/2}$ and $\delta = 4n_{io}/n_{eo}$. It is obvious that the dust charge is very sensitive to the small disturbance of ϕ . This point is very important for explaining how the variable dust charge influences the shape of solitons and solitary waves. Obviously, Eqs. (12) and (13) are complicated transcendental equations that include strongly nonlinear terms, and their numerical solutions will lead to the normalized dust charges $Z_d = \Psi/\Psi_o$. Figures 1 and 2 show that Z_d decreases as the nonthermal parameter a increases, but it requires an extra potential to reach its stable value. Also, Z_d increases as ϕ increases. For small β values, Z_d increases slightly as a increases, though it increases very rapidly to reach a higher Z_d for larger β values. As presented in the recent studies,^{6,9} there is a maximum value of δ , δ_{max} , after which the system does not permit a positive Z_d , i.e., negative charge of the dust particles. Figure 3 shows the variation of δ_{max} against a . δ_{max} decreases rapidly for small a values, thereafter it decreases gradually for higher a values. In addition, δ_{max} decreases as β increases, which agrees exactly with previous studies.^{6,9} However, Ghosh *et al.*²⁰ proved that the DA waves will suffer amplitude growth when $a > 15(1 + \beta)/(8 - 72\beta)$. For $\beta = 0.1$, this condition will lead to $a > 20.625$, which is not allowable because $0 < a < 1$.¹⁵ This declares why a damping dust charge is obtained here by increasing a . On the other hand, if one uses the usual magnetic-independent charging currents^{18,24} (which is appropriate for plasma laboratory only), one will get a dust charge number Z_d larger than that plotted in Fig. 1 with approximately the same profile (not shown).

IV. DUST-ACOUSTIC (DA) WAVES

In order to study the dynamics of small-amplitude DA solitary waves in the presence of adiabatic variation of dust charges, we derive an evolution equation from Eqs. (2)–(5), employing a reductive perturbation technique²² and introducing the stretched coordinates¹⁷ $X = \epsilon^{1/2}(x - \lambda t)$, $Y = \epsilon^{1/2}y$, $Z = \epsilon^{1/2}z$, and $T = \epsilon^{3/2}t$, where ϵ is a small parameter that measures the size of the perturbation amplitude and λ is the

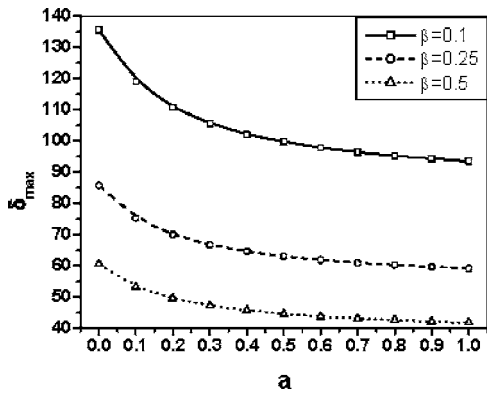


FIG. 3. δ_{max} is plotted against a for different β values with $\phi=10$.

solitary wave velocity normalized by C_d . The plasma parameters $\Theta \equiv [n_d, n_i, n_e, u_{dx}, \phi, Z_d]$ can be expanded as a power series in ε as

$$\Theta = \sum_{i=0}^{\infty} \varepsilon^i \Theta_i,$$

with $[n_{do}, n_{io}, n_{eo}, u_{dxo}, \phi_o, Z_{do}] = [1, \mu, \nu, 0, 0, 1]$, while $u_{y,z}$ are expanded as

$$u_{dy,z} = \sum_{\kappa=2}^{\infty} \varepsilon^{(\kappa+1)/2} u_{dy,z\kappa-1}.$$

Substituting these expansions into Eqs. (2)–(5), using $\psi = \psi_o Z_d$ in Eq. (12), and collecting terms of different powers of ε , in the lowest order we obtain

$$\begin{aligned} n_{d1} &= -R\phi_1, \\ u_{dx1} &= -\lambda R\phi_1, \\ u_{dy1} &= -(\lambda^2 R/\Omega)(\partial\phi_1/\partial Z), \\ u_{dz1} &= (\lambda^2/R\Omega)(\partial\phi_1/\partial Y), \\ Z_{d1} &= \gamma_1\phi_1, \\ R &= (\lambda^2 - \frac{5}{3}\sigma)^{-1}, \end{aligned} \tag{14}$$

and Poisson's equation gives the linear dispersion relation

$$\lambda = \sqrt{\frac{5\sigma}{3} + \left[\frac{4\beta(1+3a) + \delta(1-a)}{(4\beta + \delta)(1+3a)} + \gamma_1 \right]^{-1}}, \tag{15}$$

where

$$\begin{aligned} \gamma_1 &= \frac{\gamma_b}{\psi_o \gamma_a}, \quad \gamma_a = 1 + \frac{8a}{5} + \beta \left[1 - s\psi_o - \frac{8a}{5}(-3 + s\psi_o) \right], \\ \gamma_b &= (1 + \beta)(-1 + s\psi_o) + \frac{8a}{15} [1 - 2s\psi_o + 3\beta(-3 + s\psi_o)]. \end{aligned}$$

It is clear that the linear wave velocity is independent of the magnetic field, Ω . Considering both the two cases with/without dust-charge fluctuation inclusion, Figs. 4 and 5 show the variation of λ against a for different δ and β values. It is

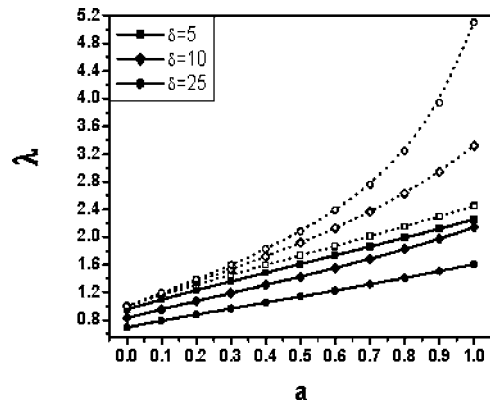


FIG. 4. λ is plotted against a for different δ values, where $\beta=0.25$, and $\sigma = 0.001$. The lower three curves correspond to varying dust charge, the upper three (dashed curves) are for the same δ values with constant dust charge.

obvious that, with the inclusion of dust-charge variation, λ increases as a increases, but it decreases as δ or β increases. In the case of constant dust-charge variation, λ increases as δ increases, however, it decreases as β increases. Generally, the effect of dust-charge variation appears to decrease the wave velocity whatever the changes occur in a , δ , or β .

For the next order in ε , we obtain a system of equations in the second-order perturbed quantities. Solving this system with the aid of (14), we finally obtain the ZK equation,

$$\frac{\partial\phi_1}{\partial T} + A\phi_1 \frac{\partial\phi_1}{\partial X} + B \left(\frac{\partial^3\phi_1}{\partial X\partial Y^2} + \frac{\partial^3\phi_1}{\partial X\partial Z^2} \right) + C \frac{\partial^3\phi_1}{\partial X^3} = 0, \tag{16}$$

where

$$\begin{aligned} A &= C \left[3R\gamma_1 - 2\gamma_2 + s^2(\mu - \nu\beta^2) - R^3 \left(3\lambda^2 - \frac{5\sigma}{9} \right) \right], \\ B &= C \left[1 + \left(\frac{\lambda^2 R}{\Omega} \right)^2 \right], \end{aligned}$$

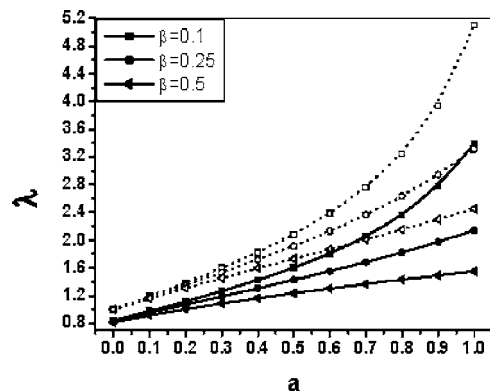


FIG. 5. λ is plotted against a for different β values, where $\delta=10$, and $\sigma = 0.001$. The lower three curves correspond to varying dust charge, the upper three (dashed curves) are for the same β values with constant dust charge.

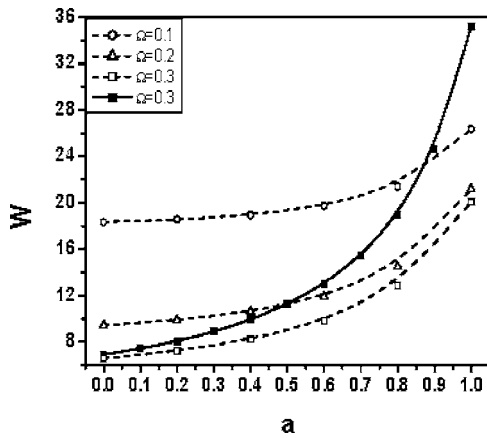


FIG. 6. W is plotted against a for different Ω values, where $\delta=10$, $\beta=0.1$, $\sigma=0.001$, $l_x=0.75$, and $u_o=0.1$. The solid curve corresponds to constant dust charge.

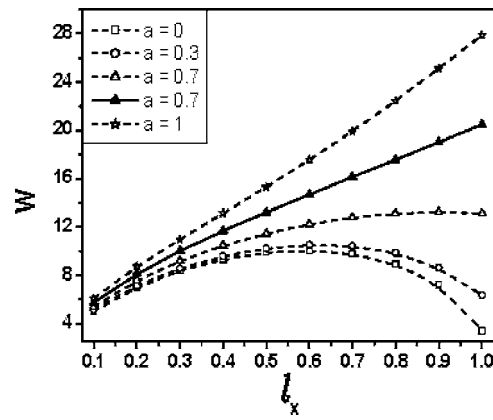


FIG. 7. W is plotted against l_x for different a values, where $\delta=10$, $\beta=0.1$, $\sigma=0.001$, $\Omega=0.2$, and $u_o=0.1$. The solid curve corresponds to constant dust charge.

$$C = (2\lambda R^2)^{-1}.$$

Using Eqs. (12) and (13), the second-order perturbed dust-charge number Z_{d2} is given by

$$Z_{d2} = \gamma_1 \phi_2 + \gamma_2 \phi_1^2, \tag{17}$$

where

$$\gamma_2 = \frac{\gamma_c}{\psi_o \gamma_a}, \quad \gamma_c = \gamma_{c1} + \gamma_{c2} + \gamma_{c3},$$

$$\gamma_{c1} = \frac{s}{30} \{ 15(-1 + \beta^2)(-1 + s\psi_o) + 8a[4 - 8s\psi_o + 3\beta^2(-3 + s\psi_o)] \},$$

$$\gamma_{c2} = \frac{s\gamma_1\psi_o}{15} \{ 8a[-2 + 3\beta^2(-3 + s\psi_o)] + 15[1 + \beta^2(-1 + s\psi_o)] \},$$

$$\gamma_{c3} = \frac{s(\beta\gamma_1\psi_o)^2}{10} [-5 + 5s\psi_o + 8a(-3 + s\psi_o)].$$

To find the stationary solution of Eq. (16), we substitute $\eta=l_x X+l_y Y+l_z Z-u_o T$ into Eq. (16), where l_x , l_y , and l_z are the directional cosine of the wave vector k along the X , Y , and Z axes, respectively, so that $l_x^2+l_y^2+l_z^2=1$. Integrating twice and using the boundary conditions

$$\phi_1(\eta) \rightarrow 0, \quad \frac{d\phi_1(\eta)}{d\eta} \rightarrow 0, \quad \frac{d^2\phi_1(\eta)}{d\eta^2} \rightarrow 0 \quad \text{as } |\eta| \rightarrow \infty, \tag{18}$$

the soliton solution of Eq. (16) is given by

$$\phi_1 = \phi_{1m} \text{Sech}^2(\eta/W), \tag{19}$$

where $\phi_{1m}=3u_o/(Al_x)$ is the amplitude, $W=\sqrt{8D/u_o}$ is the width, and $D=(l_x/2)[(l_x^2+l_y^2)B+l_x^2C]$. From the expression of ϕ_{1m} and W , it is clear that as u_o increases, the soliton amplitude increases but the width decreases. Figures 6–9 show the variation of the width W and the soliton amplitude ϕ_{1m} cor-

responding to system parameter variations. Figure 6 shows that, in case of dust-charge variation, W increases as a increases. The same effect can be observed for the constant dust charge, although W increases very rapidly for larger a values. The increase of magnetic field decreases W , however, it has no effect on the soliton amplitude. The nonlinear violence of W with l_x variation is presented in Fig. 7. For small a values, W increases/decreases for $l_x < 0.7/l_x > 0.7$. As a becomes higher, this behavior will change to a continuous increase for all l_x values. Moreover, the dust-charge variation appeared to decrease the soliton width. The soliton solution, (19), permits either rarefactive or compressive soliton passing through a critical point (will be discussed in Sec. V). Figure 8 investigates the variation of the compressive soliton amplitude ϕ_{1mc} due to system parameter variation. ϕ_{1mc} increases as β increases. For small δ , ($\delta < 10$), ϕ_{1mc} decreases very rapidly, then as δ increases, ϕ_{1mc} will have approximately a constant amplitude until δ becomes closer to δ_{max} , at which point it turns to increase again. On the other hand, Fig. 9 concerns the rarefactive soliton. It shows that the amplitude, ϕ_{1mr} , decreases very rapidly as δ increases, however, near δ_{max} it turns to increase strictly. With respect to the constant dust-charge plasma, ϕ_{1mr} decreases continuously as δ increases. Considering dust-charge variation, ϕ_{1mr} increases as β increases for small δ values, but for $\delta > 30$, the effect of β will be reversed. Although the dust-charge fluctuation will increase ϕ_{1mc} , ϕ_{1mr} will have a different response relative to the δ range under consideration (Fig. 9).

V. CRITICAL CASES

The propagation of compressive and rarefactive solitons depends on the sign of the nonlinear coefficient of the ZK equation, A , Eq. (16). Thus, the DA waves are compressive/rarefactive if $A > 0/A < 0$. This transition occurred through critical points. It can be proven that the dispersion coefficients of the ZK equation are always positive, and thus the presence of this critical behavior is due to the amplitude itself. When the nonthermal parameter a reaches a critical nonthermal parameter a_c , the nonlinear coefficient of the ZK equation vanishes, $A=0$, and the ZK equation fails to de-

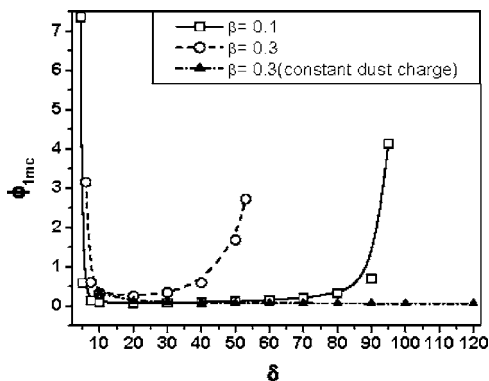


FIG. 8. ϕ_{1mc} is plotted against δ for different β values considering both varying and constant dust charge, where $a=0.7$, $l_x=0.75$, $\sigma=0.001$, and $u_o=0.1$.

scribe the system in this case. This behavior can be observed also at a critical phase velocity, λ_c , however, our concern will be focused on the former. Figure 10 shows the critical behavior of the soliton amplitude corresponding to two cases; constant and varying dust-charge variation. Figure 11 shows the dependence of a_c on δ and β variation; a_c increases as β increases. For $\delta < 20 / \delta > 20$, a_c decreases/increases as δ increases. The effect of dust-charge variation appeared to increase a_c (Figs. 10 and 11).

For describing the evolution of the system at these critical situations, one has to seek another equation suitable for describing the evolution of the system. This implies that the stretching coordinates mentioned before are not valid for this critical case, thus we will introduce a new stretching, namely,^{8,17} $X=\varepsilon(x-\lambda t)$, $Y=\varepsilon y$, $Z=\varepsilon z$, and $T=\varepsilon^3 t$, and expand

$$u_{dy,z} = \sum_{v=2}^{\infty} \varepsilon^v u_{dy,zv-1},$$

keeping the expansion of the remainder dependent variables as before. Substituting into Eqs. (2)–(5) and using $\psi=\psi_o Z_d$ into Eq. (12), then collecting terms in different powers of ε , we obtain the same relations as (14) for the lowest order of ε (coefficient of ε^2), and for the order of ε^3 , we get

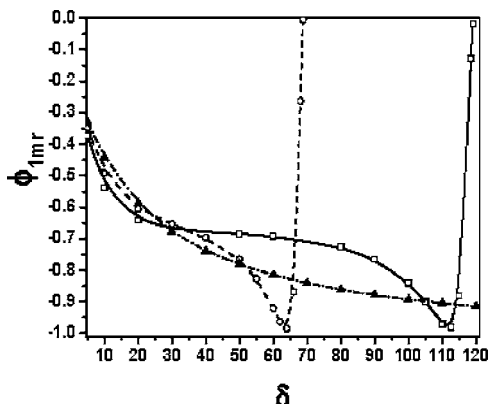


FIG. 9. ϕ_{1mr} is plotted against δ for different β values considering both varying and constant dust charge, where the figure legend and the remainder system parameters are the same as in Fig. 8.

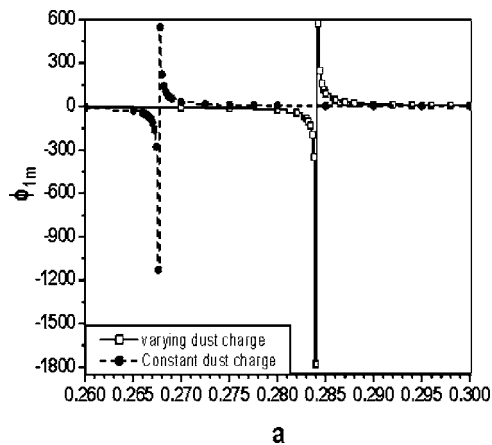


FIG. 10. ϕ_{1m} is plotted against a considering both varying and constant dust charge, where $\delta=10$, $\beta=0.1$, $\sigma=0.001$, $l_x=0.75$, and $u_o=0.1$.

$$n_{d2} = -R \left\{ \phi_2 + \frac{\phi_1^2}{2} \left[\gamma_1 + R^2 \left(\frac{5\sigma}{9} - 3\lambda^2 \right) \right] \right\}, \quad (20a)$$

$$u_{dx2} = -\lambda R \left\{ \phi_2 + \frac{\phi_1^2}{2} \left[\gamma_1 - R^2 \left(\frac{25\sigma}{9} + \lambda^2 \right) \right] \right\}, \quad (20b)$$

$$u_{dy2} = \frac{-\lambda^2 R}{\Omega} \left(\frac{\partial \phi_2}{\partial Z} + \frac{\lambda}{\Omega} \frac{\partial^2 \phi_1}{\partial X \partial Y} - \frac{40\sigma R^2}{9} \phi_1 \frac{\partial \phi_1}{\partial Z} \right), \quad (20c)$$

$$u_{dz2} = \frac{-\lambda^2 R}{\Omega} \left(-\frac{\partial \phi_2}{\partial Y} + \frac{\lambda}{\Omega} \frac{\partial^2 \phi_1}{\partial X \partial Z} + \frac{40\sigma R^2}{9} \phi_1 \frac{\partial \phi_1}{\partial Y} \right). \quad (20d)$$

If we consider the next order in ε , we obtain a system of equations which can be solved, with the aid of (14), (17), and (20), to give the following evolution equation, modified ZK equation;

$$\frac{\partial \phi_1}{\partial T} + A \frac{\partial \phi_1 \phi_2}{\partial X} + B \left(\frac{\partial^3 \phi_1}{\partial X \partial Y^2} + \frac{\partial^3 \phi_1}{\partial X \partial Z^2} \right) + C \frac{\partial^3 \phi_1}{\partial X^3} + E \phi_1^2 \frac{\partial \phi_1}{\partial X} = 0, \quad (21)$$

where

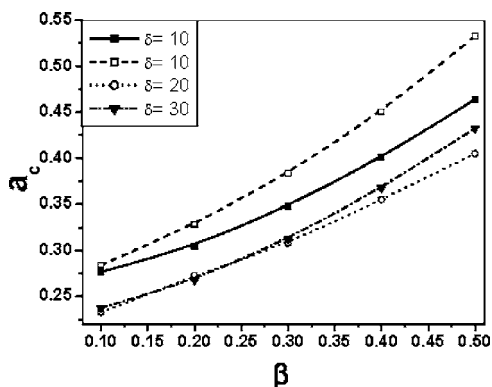


FIG. 11. a_c is plotted against β for different δ values where $l_x=0.75$, $\sigma=0.001$, and $u_o=0.1$. The solid curve corresponds to the constant dust charge.

$$E = -C \left\{ 3\gamma_3 - 4R\gamma_2 - \frac{3}{2}\gamma_1^2 R + \gamma_1 R^3 \left(9\lambda^2 - \frac{5\sigma}{3} \right) + \frac{s^3}{2} \left[\nu\beta^3 + \frac{\mu(1+15a)}{(1+3a)} \right] - \frac{5R^5}{2} \left(3\lambda^4 + \frac{58}{27}\lambda^2\sigma - \frac{5}{81}\sigma^2 \right) \right\}.$$

Using Eqs. (12) and (13), the third-order perturbed dust-charge number Z_{d3} can be given by

$$Z_{d3} = \gamma_1\phi_3 + 2\gamma_2\phi_1\phi_2 + \gamma_3\phi_1^3, \tag{22}$$

with

$$\gamma_3 = \frac{\gamma_d}{\psi_o\gamma_a}, \quad \gamma_d = \gamma_{d1} + \gamma_{d2} + \gamma_{d3} + \gamma_{d4} + \gamma_{d5} + \gamma_{d6},$$

$$\gamma_{d1} = \frac{s^2}{30} \{ 5(1 + \beta^3)(-1 + s\psi_o) + 8a[-8 + 11s\psi_o + \beta^3(-3 + s\psi_o)] \},$$

$$\gamma_{d2} = \frac{s^2\gamma_1\psi_o}{30} \{ 8a[-8 + 3\beta^3(-3 + s\psi_o)] + 15[-1 + \beta^3(-1 + s\psi_o)] \},$$

$$\gamma_{d3} = \frac{s\gamma_2\psi_o}{15} [15 - 16a - 3(5 + 24a)\beta^2 + 3(5 + 8a)s\beta^2\psi_o],$$

$$\gamma_{d4} = \frac{(s\gamma_1\psi_o)^2\beta^3}{10} [-5 + 5s\psi_o + 8a(-3 + s\psi_o)],$$

$$\gamma_{d5} = \frac{\gamma_{d4}\gamma_1\psi_o}{3}, \quad \gamma_{d6} = \frac{2\gamma_{d4}\gamma_2}{s\beta\gamma_1}.$$

Following the same procedure used before, the soliton solution of Eq. (21) is given by

$$\phi_1 = \phi_{2m} \text{Sech}(2\eta/W), \tag{23}$$

where the amplitude $\phi_{2m} = \pm \sqrt{6u_o/El_x}$. Obviously, the physically reasonable solitons correspond to the condition $E > 0$, and in this case both compressive and rarefactive solitons are also allowed to coexist.^{8,15}

On the other hand, when $A \rightarrow 0$, but $A \neq 0$, Eq. (21) would reduce to⁸

$$\frac{\partial\phi_1}{\partial T} + F\phi_1 \frac{\partial\phi_1}{\partial X} + B \left(\frac{\partial^3\phi_1}{\partial X\partial Y^2} + \frac{\partial^3\phi_1}{\partial X\partial Z^2} \right) + C \frac{\partial^3\phi_1}{\partial X^3} + E\phi_1^2 \frac{\partial\phi_1}{\partial X} = 0, \tag{24}$$

where we have used $A\phi_2 \rightarrow F\phi_1/2$. Substituting $\eta = l_x X + l_y Y + l_z Z - u_o T$ into Eq. (24), we get

$$\frac{1}{2} \left(\frac{d\phi_1}{d\eta} \right)^2 = \frac{u_o\phi_1^2}{4D} \left(1 - \frac{Fl_x}{3u_o}\phi_1 - \frac{El_x}{6u_o}\phi_1^2 \right) = -V(\phi_1, u_o), \tag{25}$$

with

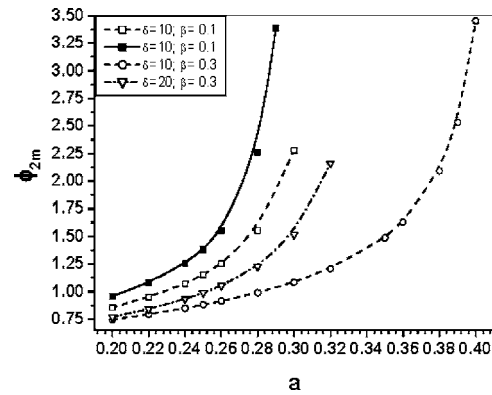


FIG. 12. ϕ_{2m} is plotted against a for different δ and β values. The upper (solid) curve corresponds to constant dust charge, with $l_x=0.75$, $\sigma=0.001$, and $u_o=0.1$.

$$V(\phi_1, u_o) = \frac{-u_o\phi_1^2}{4D} + \frac{Fl_x\phi_1^3}{12D} + \frac{El_x\phi_1^4}{24D}. \tag{26}$$

For the formation of DL,^{1,8-10} we must have

$$V(\phi_m, u_o) = 0, \quad \left(\frac{dV}{d\phi_1} \right)_{\phi_1=\phi_m} = 0, \quad \text{and} \quad \left(\frac{d^2V}{d\phi_1^2} \right)_{\phi_1=\phi_m} < 0. \tag{27}$$

The conditions (27) ensure that the particle will remain at rest at $\phi_1 = \phi_m$ and no reflection will occur. These conditions imply

$$\phi_{1m} = -F/E \text{ and } u_o = -[(F^2 l_x)/(6E)]. \tag{28}$$

Substituting for u_o into the relation (26), we obtain

$$V(\phi_1) = \frac{\phi_1^2 El_x}{24D} (\phi_1 - \phi_m)^2. \tag{29}$$

From Eqs. (25) and (29), we get

$$\left(\frac{d\phi_1}{d\eta} \right)^2 = \frac{-\phi_1^2 El_x}{12D} (\phi_1 - \phi_m)^2.$$

Then, the DL solution is

$$\phi_1 = \frac{\phi_m}{2} [1 + \tanh(\eta/W_1)], \tag{30}$$

where

$$W_1 = \frac{2}{F} \sqrt{\frac{-12DE}{l_x}}.$$

Obviously this DL solution exists only when the system parameters fulfill the condition $DE < 0$. Thus, we can get either compressive or rarefactive DA DLs, depending on the sign of F .

Figure 12 shows the validity of the soliton solution, (23), for describing the system at the critical case. It shows that the amplitude ϕ_{2m} increases/decreases as a or δ/β increases. The effect of dust-charge variation will also decrease the soliton amplitude as for the original soliton, (19).

VI. CONCLUSION

In this paper, we have analyzed analytically the properties of DA solitary waves in magnetized three-component dusty plasmas comprising of warm variational charged dust grains, nonthermal ions, and isothermal electrons. It is found that the introduction of the nonthermally distributed ions as well as the adiabatic dust-charge variation modifies significantly the DA wave properties. Using a reductive perturbation theory, a ZK equation, (16), is derived. Depending on the nonthermal parameter a , the compressive and/or rarefactive DA soliton will be created. At critical values of a , a_c , the ZK equation fails to describe the system, which forced us to seek another evolution equation adequate for describing the system. In the neighbors of a_c , a modified ZK equation with a mixed nonlinearity, third- and fourth-order nonlinearities, is derived. The solution of this evolution equation admits whether there is coexistence of both the compressive and rarefactive solitons or the creation of DL with the possibility of its two kinds, depending on the a value. The violence of DA solitary wave properties to the plasma parameters are investigated numerically, and can be summarized as follows. Although the increase of a causes a decrease of the dust charge Z_d and the maximum admitted value of δ , δ_{\max} , it increases the wave velocity λ , the soliton width W , and ϕ_{2m} . On the other hand, the effect of dust-charge variation appears to decrease λ and ϕ_{2m} , however, it increases W , ϕ_{1mc} , and a_c . For a constant dust charge, the rarefactive soliton amplitude ϕ_{1mr} decreases continuously as δ increases, although the compressive soliton ϕ_{1mc} decreases rapidly at first for $\delta < 10$, thereafter it has a constant value. In the case of dust-charge variation, however, both ϕ_{1mr} and ϕ_{1mc} decrease rapidly as δ increases, but they will increase when δ goes closer to δ_{\max} . Moreover, the solution of the modified ZK, with $A = 0$, (23), allows the coexistence of the soliton with both kinds. The effect of the parameters δ , β , and Ω on the amplitude, width, and the velocity of the DA solitary waves is also investigated in each case. The effect of another important parameter, the wave obliqueness angle on the magnetic field direction, l_x , has been investigated also. For small a values, W increases/decreases for $l_x < (0.7/l_x) > 0.7$. As a takes higher values, this behavior becomes a continuous increase for all l_x values. The soliton amplitudes, ϕ_{1mc} , ϕ_{1mr} , and ϕ_{2m} , are directly proportional to the reciprocal of l_x . In short, we can say that the soliton solution of the ZK equation, (19), is transformed at critical situation to another soliton, (23), which is characterized by the smaller amplitude and width. When the soliton disappears, DL solution, (30), is more reasonably created. The compressive/rarefactive DA DLs will be created depending on the sign of the coefficient F .

At the end, it is believed that the model and the results presented here would be applicable to specific space plasma systems such as the interaction between the solar wind with the Moon,¹⁴ in which the nonthermal ions are accelerated near the Moon due to their opposite charge to the presented dust grains. If the ions become closer to the dust grains they will contribute in the dust surface charging process. This phenomenon is associated with solitary waves and shock waves¹⁴ that are extensively discussed here. On the other

hand, from the DL properties, it is defined as a monotonic transition of the electric potential connecting smoothly two differently biased plasmas.³¹ The associated electric field is able to speed up particles in narrow spatial regions to many kilovolts. It was considered as one of the major acceleration mechanisms occurring in nature.³²

Another example is to understand the ion loss (oxygen) from Mars, which results from ion pick up caused by mass loading of the solar wind in the Martian boundary layer and ionospheric O^+ beams.¹³ As the dust grains attract the non-thermal ion particle to charge their surface, in this case, the ions seem to be captured or picked up by the dust grains, this process will cause a loss of the ion population. Thus, this paper would be very useful in interpreting ion acceleration mechanisms near the Moon and also enhance our knowledge on pickup ions around unmagnetized bodies, such as comets, Mars, and Venus.¹⁴

¹P. K. Shukla and A. A. Mamun, *Introduction to Dusty Plasma Physics* (Institute of Physics, Bristol, 2002), and references therein.

²N. N. Rao, P. K. Shukla, and M. Y. Yu, *Planet. Space Sci.* **38**, 543 (1990).

³N. D'Angelo, *Planet. Space Sci.* **38**, 1143 (1990); A. Barkan, R. L. Merlino, and N. D'Angelo, *Phys. Plasmas* **2**, 3563 (1995).

⁴E. C. Wipple, *Rep. Prog. Phys.* **44**, 1197 (1981); F. Melandsø, T. Askalsen, and O. Havnes, *Planet. Space Sci.* **41**, 321 (1993); M. R. Jana, A. Sen, and P. K. Kaw, *Phys. Rev. E* **48**, 3930 (1993).

⁵Y. N. Nejoh, *Phys. Plasmas* **4**, 2813 (1997).

⁶B. S. Xie, K. F. He, and Z. Q. Huang, *Phys. Lett. A* **247**, 403 (1998).

⁷B. S. Xie, K. F. He, and Z. Q. Huang, *Phys. Plasmas* **6**, 3808 (1999).

⁸S. K. El-Labany and W. F. El-Taibany, *Phys. Plasmas* **10**, 989 (2003).

⁹S. K. El-Labany and W. F. El-Taibany, *Phys. Plasmas* **12**, 4685 (2003); *J. Plasma Phys.* **70**, 1, 69 (2004).

¹⁰S. K. El-Labany, W. F. El-Taibany, A. A. Mamun, and W. M. Moslem, *Phys. Plasmas* **11**, 926 (2004).

¹¹J. R. Asbridge, S. J. Bame, and I. B. Strong, *J. Geophys. Res.* **73**, 5777 (1968).

¹²W. C. Feldman, S. J. Anderson, S. J. Bame *et al.*, *J. Geophys. Res.* **88**, 96 (1983).

¹³R. Lundlin, A. Zakharov, R. Pellinen *et al.*, *Nature (London)* **341**, 609 (1989).

¹⁴Y. Futaana, S. Machida, Y. Saito *et al.*, *J. Geophys. Res.* **108**, 151 (2003).

¹⁵R. A. Cairns, A. A. Mamun, R. Bingham *et al.*, *Geophys. Res. Lett.* **22**, 2709 (1995); A. A. Mamun, R. A. Cairns, and P. K. Shukla, *Phys. Plasmas* **3**, 2610 (1996).

¹⁶A. A. Mamun, *Phys. Scr.* **58**, 505 (1998).

¹⁷E. Infeld and G. Rowlands, *Nonlinear Waves, Soliton and Chaos* (Cambridge University Press, Cambridge, 1990).

¹⁸L. P. Zhang and J. K. Xue, *Chaos, Solitons Fractals* **23**, 543 (2005).

¹⁹S. Ghosh, S. Sarkar, M. Khan, and M. R. Gupta, *IEEE Trans. Plasma Sci.* **29**, 409 (2001).

²⁰S. Ghosh, R. Bharuthram, M. Khan, and M. R. Gupta, *Phys. Plasmas* **11**, 3602 (2004).

²¹J. E. Allen, *Phys. Scr.* **45**, 497 (1992).

²²H. Washimi and T. Taniuti, *Phys. Rev. Lett.* **17**, 996 (1966).

²³L. P. Zhang and J. K. Xue, *Phys. Plasmas* **12**, 042304 (2005).

²⁴A. A. Mamun and M. H. A. Hassan, *J. Plasma Phys.* **63**, 2, 191 (2000).

²⁵L. G. Laframboise and L. J. Sonmor, *Phys. Fluids B* **3**, 2472 (1991); *J. Geophys. Res.* **98**, 337 (1993).

²⁶M. Salimullah, I. Sandberg, and P. K. Shukla, *Phys. Rev. E* **68**, 027403 (2003).

²⁷V. N. Tsytovich, N. Sato, and G. E. Morfill, *New J. Phys.* **5**, 43 (2003).

²⁸V. E. Zakharov and E. A. Kuznetsov, *Sov. Phys. JETP* **39**, 285 (1974).

²⁹A. A. Mamun, S. M. Russell, C. A. Mendoza-Briceno, M. N. Alam, T. K. Datta, and A. K. Das, *Planet. Space Sci.* **48**, 163 (2000).

³⁰S. K. El-Labany, W. M. Moslem, W. F. El-Taibany, and M. Mahmoud, *Phys. Plasmas* **11**, 3303 (2004).

³¹H. Schamel, *Phys. Rep.* **140**, 161 (1986).

³²H. Schamel, *Phys. Rev. Lett.* **48**, 481 (1982).